

# THE IIUM LOW SPEED WIND TUNNEL

Fadilah Hasim, Rusman Rusyadi, Wijaya Indra Surya, Fariduzzaman  
Waqar Asrar, Ashraf Omar, J.S. M. Ali, Yulfian Aminanda, Raed Kafafy

**Abstract**— The new IIUM low speed tunnel is of a closed-loop type having a test section of 1.5m × 2.3m × 6m and a maximum speed of 50 m/s. This paper describes measurement results for initial calibration and flow characteristics of this newly constructed wind tunnel. The results show that the total pressure varies within  $0.999 \leq C_p \leq 1.003$ , the dynamic pressure varies from -0.5 to 0.4 percent from the plane mean value, the flow angularity holds within  $\pm 0.2^\circ$  and the boundary layer thickness is less than 2 percent of the equivalent hydraulic diameter of the test section.

**Keywords:** Wind Tunnel Calibration, Flow Characterization, Experimental Aerodynamics

## I. INTRODUCTION

Wind tunnels have been and will continue to be used all over the world both in research centers, academic and industrial. The new IIUM low speed wind tunnel has test section dimensions of 1.5m x 2.3m x 6m is a closed loop tunnel with a maximum air speed of 50 m/s. In order to consistently compare data, the quality of flow in the tunnel must be determined. This requires a detailed calibration process in which flow features are determined for various tunnel parameters such as airspeed, pressure variations, flow angularity and turbulence intensity.

Initial calibration tests are usually performed when a new tunnel is installed. This paper describes the results of the initial calibration tests on the empty test section, the variation in the longitudinal static pressure, the variation of the total dynamic pressure, the flow angularity, and the boundary layer thickness variation along the length of the test section.

The instruments used during the calibration have been calibrated at the Indonesian Low Speed Tunnel of LAGG/BPPT, Indonesia and can be traced back through NLR, Netherlands, and SUCOFINDO. All transducers used have been factory calibrated [5].

## II. TUNNEL CONSTANTS

The tunnel constants for the empty test section were determined by measuring static and total control pressures, temperature, static and dynamic pressures in the test section using a pitot-static tube. These measurements yield the tunnel calibration constants  $G$ , and  $H$ , which relate the tunnel control pressures to the static and dynamic pressures at the model location of the test section. The accuracy bandwidths of the pressure measurements have been determined using the maximum uncertainty in the pressure measurements for the first series of measurements and for all further tests were determined using ISO 7066-2 [4].

The tunnel reference parameters are determined using instruments installed in the contraction section. These are: (four) total pressure probes ( $p_t$ ), (two) temperature probes ( $T_c$ ) and (four) static pressure ( $p_s$ ) taps. The four static pressure taps were installed at the four walls at the end of the contraction. Four total pressure probes were installed at the four walls of the contraction and two temperature probes were installed at the floor and ceiling at the beginning of the contraction.

The control static pressure is defined as the average of the four static pressure at the end of the contraction, i.e.,

$$p_c = \frac{1}{4}(p_{s1} + p_{s2} + p_{s3} + p_{s4}) \quad (1)$$

Control differential pressure is an average of differential pressures used for the tunnel control. This pressure is defined as the average of two total pressures minus the average of the four static pressure (control static pressure), i.e.,

$$\Delta p_c = \frac{1}{2}(p_{t1} + p_{t2}) - \frac{1}{4}(p_{s1} + p_{s2} + p_{s3} + p_{s4}) \quad (2)$$

Fadilah Hasim, Wijaya Indra Surya, and Fariduzzaman are with the Laboratory for Aero, Gas dynamics and Vibration LAGG (BPPT), Indonesia, Rusman Rusyadi is with the Research Center for Calibration, Instrumentation and Metrology (KIM) LIPI, Indonesia.

Waqar Asrar, Ashraf Omar, J. S. M. Ali, Yulfian Aminanda, and Raed Kafafy, are with the Dept. of Mechanical Engineering, International Islamic University Malaysia, IIUM, P.O.Box 10, 50728 Kuala Lumpur, Malaysia (Phone: ++6(03)61964590, Fax: ++6(03)61964455, e-mail: waqar@iiu.edu.my).

The dynamic and the static pressures in the empty test section can be expressed in terms of the tunnel control pressures as follows. The dynamic pressure in the empty test section is

$$q_0 = p_c \left\{ G_0 + G_1 \left( \frac{\Delta p_c}{p_c} \right) + G_2 \left( \frac{\Delta p_c}{p_c} \right)^2 \right\} \quad (3)$$

The static pressure in the empty test section is

$$p_0 = p_c \left\{ H_0 + H_1 \left( \frac{\Delta p_c}{p_c} \right) + H_2 \left( \frac{\Delta p_c}{p_c} \right)^2 \right\} \quad (4)$$

Here,  $G_0 \sim G_2$  and  $H_0 \sim H_2$  are the calibration constants obtained from the calibration test. Empty test section calibrations were performed to find the relation between tunnel control pressures and the pressures at the center of the test section. The first series of tests were carried out. The tunnel constants were obtained, pressure distributions were measured. The results were within acceptable margins. However the test results for flow angularity showed some abnormal behavior in both pitch and yaw. Several actions such as sanding of the trailing edges of the honeycomb panels and tightening up the fine and coarse screens were then performed for improvement. Following the efforts to improve the flow quality mentioned above, a second series of calibration tests on the empty test section were carried out to measure the new tunnel constants.

The instruments and procedures of calibration were the same as in the first calibration except the transducer used for measuring pitot static pressure. To improve the measurement stability, static pressure was not directly measured by absolute transducer. Static pressure port of the pitot tube was connected to tunnel control static pressure  $p_{s4}$  through the differential pressure transducer, and static pressure  $p_{s4}$  used for tunnel control pressure was measured by an high accuracy absolute transducer [5]. Thus the static pressure of the pitot becomes:

$$P_{ref} = P_{s4} + (P_{ref} - P_{s4}) \quad (5)$$

This configuration was chosen (instead of using the absolute transducer  $p_{i3}$  to measure pitot static pressure) to improve the accuracy of measurement. Total and static pressure ports of the pitot tube were connected to differential transducer for  $\Delta p_{c3}$  as in the first calibration. The tunnel was run from a fan RPM of 100 to a maximum RPM of 575 in steps of 25 and then descending back to an RPM of 100 in steps of 25. After carrying out the pressure measurements (each measurement was averaged from 30 samples acquired using a 0.5 second sampling time for each sample) and analysis, the following relationships were obtained.

The dynamic pressure in the empty test section follows:

$$q_0 = p_c \left\{ -0.000032 + 0.977623 \left( \frac{\Delta p_c}{p_c} \right) - 0.586890 \left( \frac{\Delta p_c}{p_c} \right)^2 \right\} \quad (6)$$

and the static pressure in the empty test section obeys:

$$p_0 = p_c \left\{ 0.999725 + 0.020288 \left( \frac{\Delta p_c}{p_c} \right) + 0.550108 \left( \frac{\Delta p_c}{p_c} \right)^2 \right\} \quad (7)$$

### III. LONGITUDINAL STATIC PRESSURE GRADIENT

The longitudinal static pressure distribution in the test section was established by using a static pressure pipe having a diameter of 0.06 m (less than 1 percent cross section blockage of the test section). The pipe measures 6 m long with 3 static pressure ports each at 14 stations along the length. The pipe was installed in the center of the test section using wires of 1 mm diameter (Fig. 1).



Fig. 1 Installation of static pipe in the wind tunnel.

Measurements for longitudinal static pressure distribution were performed at speeds of 30, 40 and 50 m/s. The pressure distribution is usually expressed in terms of pressure coefficient,  $C_p$ , which is defined as

$$C_p = \frac{p(x) - p_0}{q_0} \quad (8)$$

Where  $p(x)$  is pressure at  $x$  position,  $p_0$  and  $q_0$  are the static and dynamic pressures at the center of the test section respectively. The static and dynamic pressures at the center of the test section can be determined from tunnel reference using calibration factors.

The longitudinal variation of  $C_p$  is shown in Fig. 2. The results show that the pressure variation on most of the turn table length is approximately within the limits of  $\pm 0.003$ . This satisfies the specified values of longitudinal static pressure variation for an aeronautical wind tunnel [3].

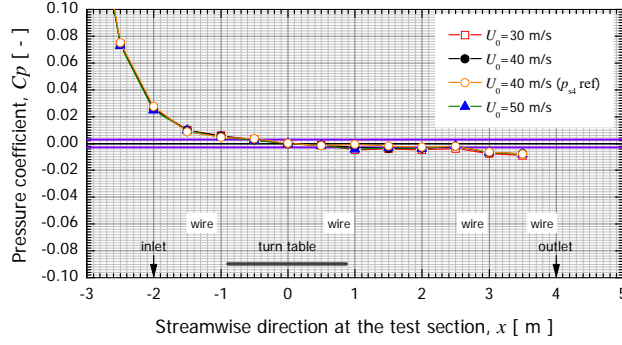


Fig. 2 Longitudinal variation of pressure coefficient.

#### IV. VARIATION IN TOTAL AND DYNAMIC PRESSURE ACROSS JET

The variation in the total and dynamic pressures was established at a speed of 40 m/s at three cross sections (planes) in the longitudinal directions. The measurements were corrected for the rise in temperature during the tests.

Coefficient pressure for total head is expressed as follows:

$$C_{p_t} = \frac{p_t - p_c}{q_c} \quad (9)$$

Where  $p_c$  and  $q_c$  are static and dynamic pressures at the center of measurement plane. In actual measurement,  $p_t$  cannot be measured using an absolute transducer, because it requires a very fine resolution that absolute transducer cannot provide. Thus two differential transducers were used to measure  $(p_t - p_{s4})$  and  $(p_c - p_{s4})$ . The coefficient of total pressure then can be expressed as

$$C_{p_t} = \frac{(p_t - p_{s4}) - (p_c - p_{s4})}{q_c} \quad (10)$$

Total pressure distribution can be also expressed by its deviation of the coefficient in percent from the mean coefficient of total pressure of the measured plane, i.e.,

$$\delta C_{p_t} = \frac{(C_{p_t} - C_{p_t-mean})}{C_{p_t-mean}} \times 100\% \quad (11)$$

The measurement results for the total pressure variations at a few locations are shown in Figs. 3 and 4. The variation of the total pressure coefficient was found to be approximately in the limit  $0.999 \leq C_{p_t} \leq 1.003$  for all measured planes.

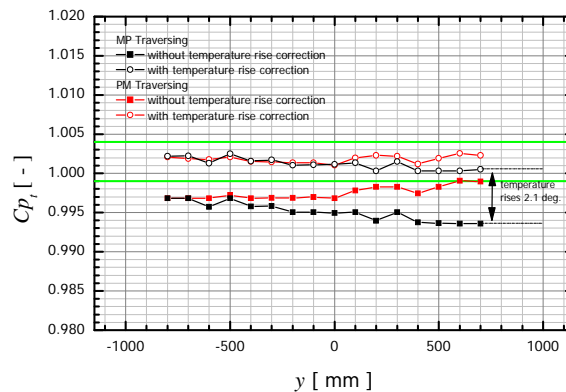


Figure 3 Variation of total pressure along y direction at  $x = 1.880$  m,  $z = 0.500$  m.

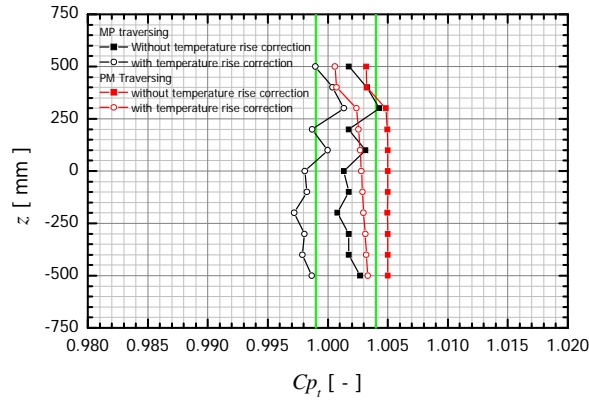


Figure 4 Variation of total pressure along the z direction at  $x = 1.880$  m,  $y = 0.700$  m.

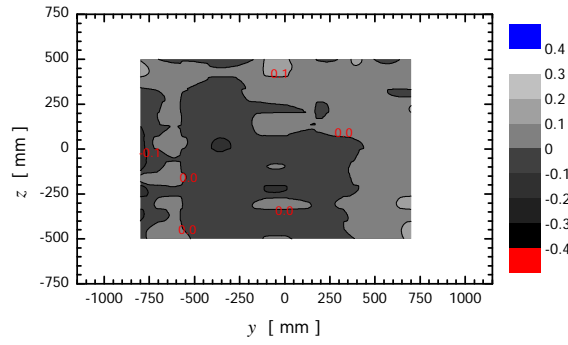


Figure 5 Deviation of total pressure coefficient (percent from the plane mean) at plane C,  $x = 1.880$  m.

Variation of the dynamic pressure is shown for a cross section in Fig. 5. The dynamic pressure variation is

$$\frac{dq}{q_{mean}} = \frac{q - q_{mean}}{q_{mean}} \quad (12)$$

The variation in the dynamic pressure from the mean was found to be from -0.4 to 0.4 percent in the upstream section of the test section. This variation was from -0.5 to 0.3 percent near the midsection and from -0.3 to 0.2 percent at the downstream section. The variations are within the usual range of 0.4 to 0.6 percent for general-purpose wind tunnels [2].

## V. FLOW ANGULARITY

A calibrated yaw head probe was used to establish the flow angularity variation in the test section. Measurements were made at three sections located in the longitudinal direction at an air speed of 40 m/s. The measurements were corrected for the rise in temperature during the test. Sample results of the measurements are shown in Figs. 6 and 7. The figures indicate that the flow angle variation across the jet is less than  $\pm 0.2^\circ$ . This satisfies the allowable variation for an aeronautical wind tunnel [2].

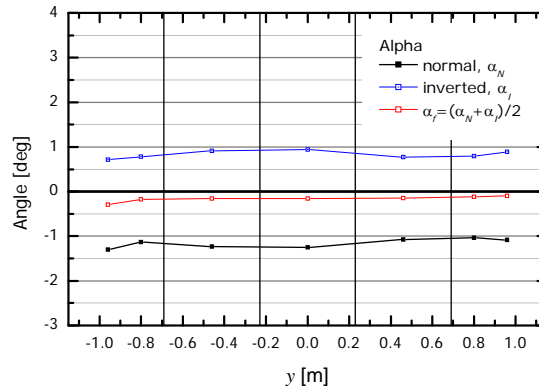


Figure 6 Flow angularity in pitch in the y direction, at  $x = -1.030$  m,  $z = 0.550$  m.

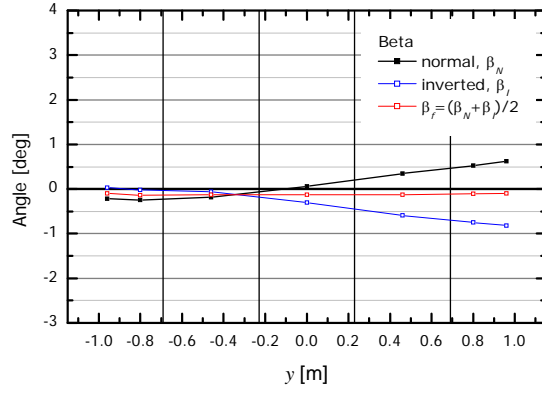


Figure 7 Flow angle variation in yaw in the y direction, at  $x = -1.030$  m,  $z = 0.550$  m

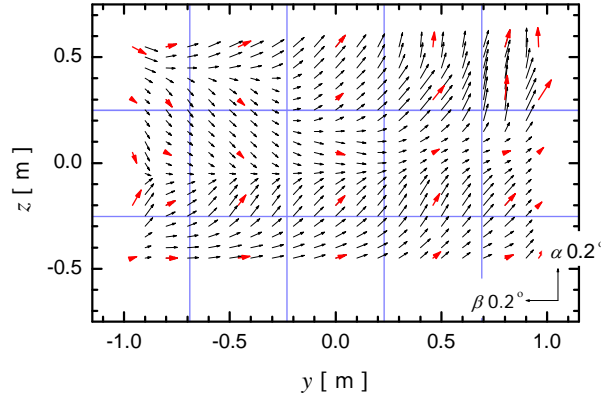


Figure 8 Cross-flow plot of airstream at  $x = 1.880$  m

Figure 8 shows a compiled cross-flow plot of airstream at the cross section of  $x = 1.880$  m. The red arrows in the figure represent the measurements points, and the flow pattern is obtained using multivariate interpolation from these measurement points. The blue grids in the figure correspond to the layout of the honeycomb panels in the settling chamber. The flow pattern shows that the flow in the test section has the upflow ( $\alpha$  positive) and cross-flow ( $\beta$ ) negative. But as can be compared to the scale in the figure both upflow and cross-flow are less than  $\pm 0.2^\circ$ .

## VI. BOUNDARY LAYER GROWTH

The boundary layer thickness was measured using a boundary layer rake. The rake consists of one static pressure port at the top and twenty total pressure probes, so that the dynamic pressures profiles which determine velocity profiles can be derived. Velocity profiles are then normalized with the boundary layer rake tip velocity, to force the velocity ratio at the boundary layer rake tip to be 1.0 [1]. Boundary layer thickness defined as the distance from the wall of the test section at which the velocity ratio equals to 0.990,

Measurements were performed on four walls: floor, port wall, starboard wall and ceiling. Each wall has three measurement points which represented upstream (A), center (B) and downstream (C) regions of the test section. The measurement points at each wall are adjusted according to the structure of the test section. The measurements were carried out at airspeeds of 30, 40 and 50 m/s.

Measurement results for boundary layer thickness are shown in Figures 9 and 10. In the figures, the distance from the wall,  $y$  or  $z$ , is normalized by the equivalent hydraulic diameter,  $D_h$ , and velocity,  $U$ , is normalized by the rake tip velocity,  $U_{max}$ . The equivalent hydraulic diameter,  $D_h$ , is defined by

$$D_h = \frac{4A}{2H + 2W}$$

Where  $A$  is the area of the cross-section,  $H$  and  $W$  are height and width of the test section respectively.

The figures show the boundary layer thickness on the floor and starboard around  $x = 0.000$  (the model location) is less than 2 percent of equivalent hydraulic diameter. The velocity profiles are very consistent with turbulence boundary layer development, i.e., the boundary layer thickness increase as flow goes downstream. The boundary layer at the ceiling develops a little faster and shows slight irregularity. But it is still very acceptable. As a whole, these boundary layer data show that the flow in the test section can be considered as separation free.

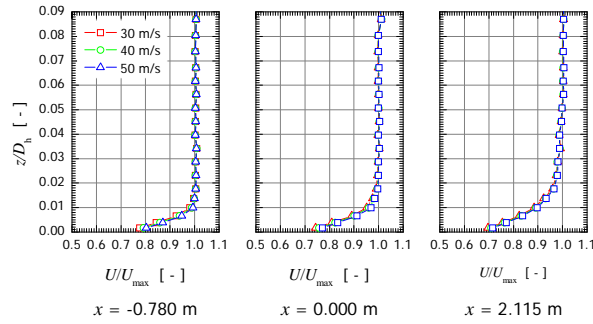


Fig. 9 Velocity profiles on the floor of the test section.

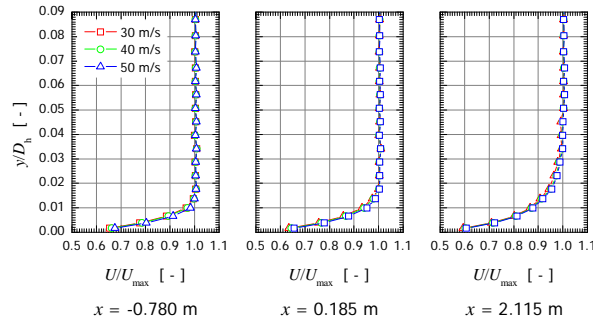


Fig.10 Velocity profiles on the starboard wall of the test section.

## VII. CONCLUSIONS

A series of measurements has been performed for initial calibration and flow field characteristics of new IIUM low speed tunnel. The following conclusions could be drawn:

- The longitudinal static pressure variation on most of the turn table length is approximately within  $\pm 0.003$ .
- The total pressure shows that  $0.999 \leq C_{p_t} \leq 1.003$  holds for all measured planes.
- The dynamic pressure varies from  $-0.5$  to  $0.4$  percent from the plane mean value.
- The variation of flow angle across the jet is less than  $\pm 0.2^\circ$  for both pitch and yaw angles.
- The boundary layer growth is very reasonable. The boundary layer thickness around the model location is less than 2 percent of the equivalent hydraulic diameter.

## VIII. REFERENCES

- [1] AIAA *Recommended Practice – Calibration of Subsonic and Transonic Wind Tunnels*, AIAA R-093-2003, Reston VA, 2003.
- [2] Barlow, J. B., Rae (Jr.), W. H., Pope, A., *Low Speed Wind tunnel Testing*, Wiley-Interscience, 1999.
- [3] Eckert, D., “First Performance and calibration Tests”, Seidel, M. (Ed), *CONSTRUCTION 1976-1980 Design Manufacturing calibration of the German-Dutch Wind tunnel (DNW)*, Noordoostpolder, 1982.
- [4] International Organization for Standardization, *Assessment of uncertainty in the calibration and use of flow measurement devices – Part 2: Nonlinear calibration relationships*, ISO 7-66-2, 1988.
- [5] S&V Teknik Sdn Bhd. & Aero Engineering, *Initial Calibration Tests – IIUM Wind Tunnel*, 2008.